

10.2 EMERGENCY DISPERSION FORECASTS FOR EAST TENNESSEE: HOW BEST TO UTILIZE WRF?

Ronald Dobosy¹ and David John Gagne²

NOAA Air Resources Laboratory, Atmospheric Turbulence and Diffusion Division
Oak Ridge, Tennessee

1. INTRODUCTION

It is an ongoing dream to be able to give the first responder to a hazardous atmospheric spill a better wind and mixing estimate than simply a guess based on the local wind observed at the surface. In complex terrain the multiple opportunities for aerodynamic mischief are well known (*e.g.*, Bowen *et al.*, 2000) and often only qualitatively simulated by numerical models. With the explosion of computer power and the accompanying wide availability of sophisticated mesoscale atmospheric models come opportunities for continually improving the ability of models to provide useful locally optimized answers. The Weather Research and Forecast Model (WRF) has been running at NOAA/ATDD for about two years (ATDD, 2010), and the forecasts for East Tennessee have been archived. Concurrently, ATDD's Regional Atmospheric Monitoring and Analysis Network (RAMAN) has been collecting and archiving measurements of wind and temperature. These provide real-world information streams from which to evaluate and enhance the utility of WRF to those first responding to hazardous atmospheric spills.

This abstract reports a first assessment of the performance of ATDD's baseline configuration of WRF in East Tennessee. It focuses on WRF's simulation of mesoscale atmospheric conditions. If the mesoscale forecast lacks fidelity, the local-scale forecast will scarcely be of use.

2. TERRAIN IN EAST TENNESSEE

Figure 1 shows East Tennessee to be dominated by a broad valley 50 km wide, 450 km long draining to southwest, with depth ranging from 75 m at Kingsport, to 250 m at Chattanooga. Its "rim," the depth it could be filled with water if its southern end were closed, is about 450 m above mean sea level (MSL). Since the valley has no real name, it will be called simply "the Valley." Great Smoky Mountains National Park is on the highest mountains along the North Carolina border straight south from Morristown. The terrain

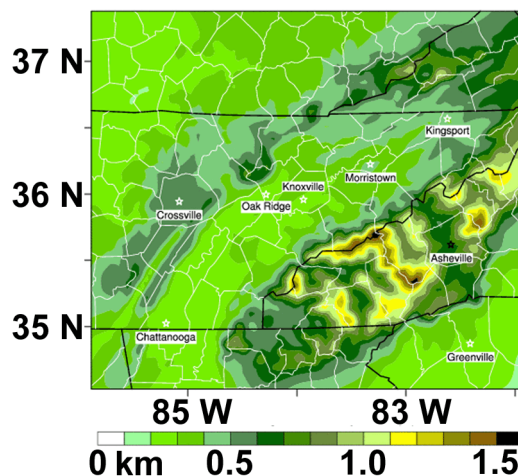


Figure 1: East Tennessee Terrain Elevation.
Color changes every 100 m.

features depicted in Figure 1 are smoothed sufficiently to allow sampling on a discrete grid of 3.3-km spacing without spatial aliasing. This is the terrain visible to our configuration of WRF. Significant to the region but invisible to WRF are long parallel ridges which corrugate the Valley floor. These are 70 m to 100 m high, separated by about 2 km and are quite apparent to the people of East Tennessee, who live and work primarily on the Valley floor between them. From multiple studies of mesoscale flow in East Tennessee three wind regimes have been identified: 1) flow external to the Valley (geostrophic wind), 2) flow at ridge-top level, and 3) flow between the ridges.

3. INFORMATION STREAMS

The information streams on which this assessment is based come in three types. **Data** are direct measurements or measurements "minimally" processed. **Analyses** combine a prior model forecast with current atmospheric observations to establish an optimal estimate of the atmosphere's current state. **Forecasts** are pure results of a model run. These three streams are a powerful resource for evaluation, improvement, and testing of our implementation of WRF. For this first look the three types of information are matched in time but not in space.

¹Oak Ridge Associated Universities, assigned to NOAA/ATDD

²NOAA Ernest F. Hollings Fellow

3.1 Data

3.1.1 RAMAN:

The RAMAN Network (ATDD, 2010) measures wind, temperature, relative humidity, and precipitation at 16 sites. The sites are in three types of locations. Five are on mountain tops, 700 m to 1500 m MSL; eight are on ridge tops, 350 m to 440 m MSL; and two are on the Valley floor, 280 m and 290 m MSL. All sites are elevated above the trees on fire towers or on dedicated towers spread over a radius of about 100 km around Knoxville, but somewhat biased toward the west side of the Valley.

3.1.2 Geostrophic Wind:

Technically, the external geostrophic wind is “analysis” since it is determined from the vector-average pressure gradient, uniformly weighted, over a circular region 500 km in diameter at 1500 m MSL in the outer (10 km) mesh of the RUC/WPS analysis described below. It is considered “minimally” assimilated, however, because its altitude is above the main influences of local terrain, and its scale, by virtue of the average, is sufficiently large to be meaningfully constrained by the observations assimilated into the RUC/WPS analysis.

3.2 Analysis

Analysis has a technical meaning in the context of the three information streams considered here. Historically it named the subjective process of blending data with the analyst’s experience to identify the coherent patterns that enable forecasting (*e.g.*, Saucier, 1955). By analog, the current “objective” analysis (*e.g.*, Benjamin *et al.*, 2004) provides the initial state from which numerical forecasts begin. The first guess of this Bayesian process comes usually from a prior forecast valid at the current time. This field is improved by blending with new observations according to the confidence in these observations relative to the confidence in the first guess.

A major benefit to mesoscale modeling comes from the availability of gridded analysis and forecast fields from continental- and global-scale models run operationally by weather services such as the US National Centers for Environmental Prediction (NCEP). Without such products, regional mesoscale modeling would have no knowledge of the ongoing state of the atmosphere, including the geostrophic wind mentioned above, hence no utility to real-time estimates of the wind and dispersion.

During the time of this study NCEP ran the Rapid Update Cycle Model (RUC, Benjamin *et al.*, 2004) out

to six hours, restarting every hour. Every third run continued to 12 hr. Of these longer runs ATDD used 03Z, 09Z, and 18Z to start and to bound 12-hr runs of WRF. The RUC provided grid fields at 20-km spacing; the WRF implementation used a two-level nest, the outer mesh of which had 10 km grid intervals, the inner mesh 3.3 km. This inner mesh exactly covers the region depicted in Figure 1. The WRF Preprocessing System (WPS, NCAR 2009) provides the necessary translation from RUC to WRF, interpolates the fields to the finer mesh, and adjusts them for the finer resolution of terrain. This produces the RUC/WPS analysis mentioned earlier. No new data are assimilated at this stage. In particular the RAMAN data are entirely independent of the analysis and forecast streams.

The analysis stream used here is a series of analyzed wind fields, each valid at 09 UTC, (0400 in Oak Ridge). A vector-average wind is taken for each day of calendar year 2009 at 10 m above WRF’s ground level, which is depicted in Figure 1. The average includes all points that are below the valley’s rim (450 m MSL) and within an ellipse that covers the Valley and part of the surrounding upland.

3.3 Forecast

The WRF V2.2 model was initialized three times per day by the RUC/WRF analysis on the two-level nest described above and run out to 12 hr. It used the default physics and two-way interaction between the nest levels. Boundary conditions on the outer mesh were derived from the 12-hr RUC forecasts keeping the mesoscale WRF aware of the forecast of atmospheric state in the larger world.

The forecast stream used here is series of six-hour forecasts started at 03 UTC (2200 in Oak Ridge) and valid at 09 UTC (0400 next morning in Oak Ridge), the same time of day as the analysis series. The forecast stream contains the same vector average wind over the Valley as does the analysis stream.

4. MESOSCALE ATMOSPHERIC PATTERN: VALLEY STEERING

For this assessment of the fidelity of our implementation of WRF in simulating mesoscale atmospheric features of East Tennessee we chose the pattern called valley steering. The pattern, well studied in this area (Nappo, 1977; Whiteman and Doran, 1993; Birdwell, 1996; Eckman, 1998), concerns the interaction of the flow in the valley with that above and beyond the valley. The schematic (Figure 2) from Whiteman and Doran (1993) identifies four modes of interaction based on the direction and strength of the wind within and above the valley.

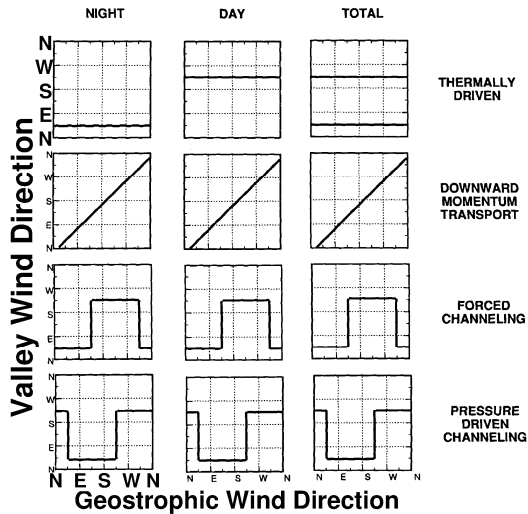


Figure 2: Four modes of valley steering with the valley oriented as in East Tennessee; adapted from Whiteman and Doran (1993)

In *thermally driven* flow the external wind has minimal influence on the valley, usually because it is weak. Wind in the valley is thus controlled by the mountain-valley circulation. If the diurnal heating and cooling are sufficiently strong, the flow will be upvalley (from southwest) in the day and will drain downvalley (from northeast) at night, regardless of the wind direction aloft.

Downward momentum transport or *unchanneled flow* is the opposite extreme. The external flow dominates as if the valley weren't there. The valley wind follows the wind aloft except for some deflection toward large-scale low pressure reflecting the Eckman balance. In the Northern Hemisphere, this will be to port (left facing downwind).

Forced channeling involves contributions from both the valley and the outside world with the external flow approximately aligned with the valley's axis. Air in the valley is guided by the sidewalls to become more directly parallel to the valley's axis, from northeast or from southwest, whichever better aligns with the flow aloft.

Pressure-Driven Channeling also involves contributions from both valley and aloft, but the external flow is approximately perpendicular to the valley's axis. Since the flow aloft is close to geostrophic balance, the pressure-gradient force in the Northern Hemisphere will be to its port side and perpendicular. That is, it will be generally aligned with the valley axis and will accelerate the valley air along the axis in the general direction of large-scale low pressure. With northwesterly geostrophic wind, the valley flow is accelerated from southwest. With southeasterly geostrophic wind, the valley air is accelerated from northeast.

5. PRELIMINARY RESULTS

The results are presented as scatter plots. The valley wind direction is plotted as a function of the external geostrophic wind direction, following the form of the individual panels of Figure 2. All plots use information from one calendar year, 2009, and apply to 09 UTC (0400 in Oak Ridge)

5.1 Data

Figure 3 presents data only. The wide, faint cyan lines depict the orientation of the Valley, with drainage

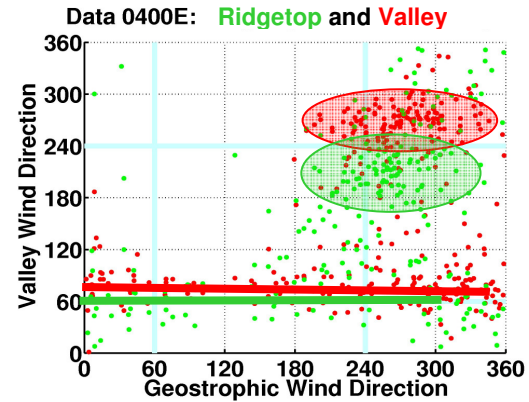


Figure 3: Scatter plot of measured Valley wind direction as function of external wind direction (text section 3.1.2). Each dot is an hour average at 09 UTC on a particular day in calendar year 2009. See text for details.

from the northeast, actually 60°. The red dots represent daily wind observations at 09 UTC from a single station on the valley floor in ATDD's compound. These winds tend to form two clusters, identified by eye and by windrose to come from the east or the west. This matches local drainage around the site but is 30° clockwise from the general Valley's orientation. The strongly local character of wind between the

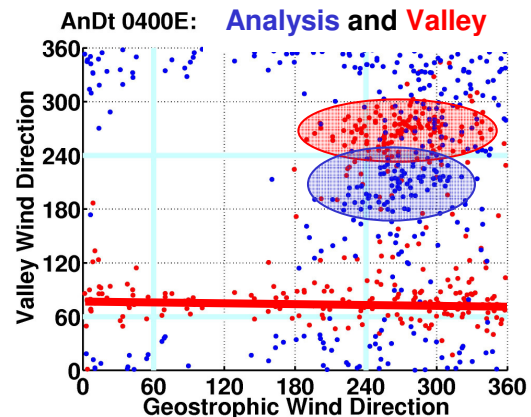


Figure 4: As Figure 3, showing measured wind on Valley floor, but with analysis-derived valley-average wind at 10 m above ground from 09 UTC each day.

ridges and the value of additional valley-floor stations beyond the two currently operating are evident. Wind from the east, the local direction of drainage, can be observed with any wind direction aloft, consistent with the thermally forced pattern of valley flow. West wind is not observed on the Valley's floor unless the flow aloft has a westerly component. Any of the remaining three modes of valley steering could produce this result. Identifying them individually awaits more detailed examination.

The green dots represent the daily vector-average direction of wind measured at 09 UTC at seven ridgetop sites. Data from the eighth site were rejected from this first look but will be included in more thorough examination later. These winds are more broadly scattered, probably reflecting greater freedom than that found between the parallel ridges. Two clusters are evident. As on the Valley floor, easterly winds appear with all wind directions aloft, consistent with the thermally forced pattern, but their direction is now aligned with the general Valley. Finding drainage up to 100 m above the valley floor is significant for modeling. The other cluster, as on the Valley floor, appears only when the wind aloft has a component from the west. Its direction, however, differs from that found at the Valley-floor site by more than 45°.

5.2 Analysis

Figure 4 compares the analysis with data from the site on the Valley floor. The winds of the analysis show scatter, but also again two main clusters. The cluster apparently analogous to the drainage flow from the east, however, is instead centered on north, consistent neither with the measurements nor with the direction of drainage flow in the general valley. The cluster which appears to match the forced flow from the west is centered instead on southwest.

Figure 5 compares the analysis with the vector-average direction over the seven ridgetop sites. The analysis winds clustered about north are no better

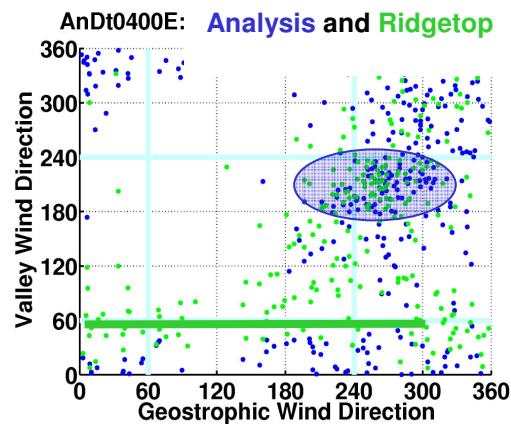


Figure 5: Wind from 09 UTC analyses as Figure 4, but with measured ridge-top wind.

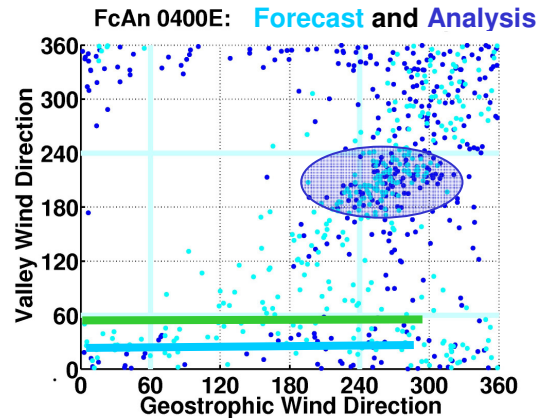


Figure 6: As earlier figures but comparing valley-average wind from 09 UTC analyses with six-hour forecast valid at 09 UTC. Green bar, taken from Figure 5, represents measured ridgetop wind.

match for these than for the observations on the valley floor. However, a good match, at least in aggregate is found between the analyzed and measured winds from the southwest.

5.3 Forecast

Figure 6 compares the six-hour forecast with the analysis. The cluster which appears analogous to the drainage flow is centered on 30° (darker cyan line), still seriously at variance with the measured result indicated by the green line reproduced from Figure 5. However, the forecast of valley-averaged wind influenced by the flow aloft, is well matched with the corresponding analysis, at least in aggregate, and perhaps even better matched with the data in Figure 5.

6. CONCLUSIONS

The base-line implementation of WRF at ATDD, initialized and bounded by RUC/WPS analysis matches the ridge-top measurements of nocturnal flow in the Valley in East Tennessee with an appreciable degree of skill both in analysis and in six-hour forecast as long as the valley wind is influenced by the geostrophic wind aloft. In thermally forced drainage flow, however, both forecast and analysis are at major variance with ridge-top measurements.

The inability of 3.3 km grid spacing to resolve the corrugating ridges on the valley floor was found to be a serious handicap under all conditions at night (09 UTC). The measured flow at the station on the Valley floor was entirely misrepresented by both analysis and forecast. This is a major problem, since the people primarily live and work on the Valley floor between the ridges.

7. NEXT STEPS

The valley average of the analyzed and forecast wind at 10 m above WRF-perceived ground may not properly represent the vector-average wind over the ridgetop sites. In particular, the RAMAN sites' locations are biased toward the west side of the Valley. Further analysis is indicated.

Additional fields, including wind speed, temperature, and pressure, available in analysis and forecast, will support assessment of the validity of the model's physics. This will likely include examination in terms of the several modes of externally influenced valley flow.

There may be multiple approaches to addressing the flow between the ridges. The limited range of flow direction between these corrugations makes mesoscale model-output statistics (MOS) attractive. These have been developed from the three data streams. The results of current efforts are reported by Gagne and Dobosy (2010). Since the corrugations are resolvable by the current WRF grid in two out of the three spatial dimensions, modification of physical models of the surface-layer and boundary-layer may sidestep the need to resolve these corrugations fully, thus avoiding further horizontal refinement of the grid.

8. REFERENCES

ATDD, 2010: Atmospheric Turbulence and Diffusion Division, NOAA, <http://www.atdd.noaa.gov/>, accessed 2010 February

Benjamin, S.G., G.E. Grell, J.M. Brown, T.G. Smirnova, 2004: Mesoscale weather prediction with the RUC hybrid isentropic-terrain-following coordinate model. *Monthly Weather Review* **132**, 473 – 494

Birdwell, K.R., 1996: A Climatology of Winds Over a Ridge An Valley Terrain within the Great Valley of

Eastern Tennessee. Masters Thesis, Murray State University, Murray, Kentucky, 258 pg.

Bowen, B.M., J.A. Baars, and G.L. Stone, 2000: Nocturnal Wind Direction Shear and Its Potential Impact on Pollutant Transport. *Journal of Applied Meteorology* **39**, 437–445

Eckman, R.M. 1998: Observations and Numerical Simulations of Winds within a Broad Forested Valley. *Journal of Applied Meteorology* **37**, 206–219

Gagne, D. J., and R.J. Dobosy, 2010: An evaluation of WRF model output statistics techniques in eastern Tennessee. American Meteorological Society, 16th Conference on Air Pollution Meteorology, paper 12.1 http://ams.confex.com/ams/90annual/techprogram/paper_158494.htm accessed 2010 February

Nappo, C.J. 1977: Mesoscale Flow over Complex Terrain during the Eastern Tennessee Trajectory Experiment (ETTEX). *Journal of Applied Meteorology* **16**, 1186–1196

NCAR, 2009: ARW Version 3 Modeling System Users' Guide. National Center for Atmospheric Research, Mesoscale and Microscale Meteorology Division, Boulder CO, 310 pg, available at http://www.mmm.ucar.edu/wrf/users/docs/user_guide_V3.1/contents.html accessed 2010 February

Saucier, W. J., 1955: *Principles of Meteorological Analysis*. University of Chicago Press, Chicago IL, ISBN 0-226-73533-8, 438 pg.

Whiteman, C.D. and J.C. Doran, 1993: The relationship between overlying synoptic-scale flows and winds within a valley. *Journal of Applied Meteorology* **32**, 1669 – 1682.